Journal of Biomedical Optics 14(1), 014030 (January/February 2009)

Multipoint fluorescence correlation spectroscopy with total internal reflection fluorescence microscope

Yu Ohsugi
Masataka Kinjo
Hokkaido University
Laboratory of Molecular Cell Dynamics
Faculty of Advanced Life Science
Sapporo 001-0021, Japan

Abstract. We report simultaneous determination of diffusion coefficients at different points of a cell membrane using a multipoint fluorescence correlation spectroscopy (FCS) system. A system carrying seven detection areas in the evanescent field is achieved by using seven optical fibers on the image plane in the detection port of an objective-type total internal reflection FCS (TIR-FCS) system. Fluctuation of fluorescence intensity is monitored and evaluated using seven photomultiplier tubes (PMTs) and a newly constructed multichannel correlator. We demonstrate simultaneous-multipoint FCS, with a 3-μs time resolution, to investigate heterogeneous structures such as cell membranes and membrane-binding molecular dynamics near glass surfaces in live cells. © *2009 Society of Photo-Optical Instrumentation Engineers.* [DOI: 10.1117/1.3080723]

Keywords: fluorescence spectroscopy; correlation; total internal reflection fluorescence microscope; cell membranes; molecular dynamics.

Paper 08338LRR received Sep. 18, 2008; revised manuscript received Dec. 23, 2008; accepted for publication Dec. 30, 2008; published online Feb. 24, 2009.

1 Introduction

Fluorescence correlation spectroscopy[1] (FCS) is a powerful tool to investigate molecular behavior such as diffusional mobility, photophysical properties, and reaction kinetics *in vitro*[2] and *in vivo*.[3] In spite of their wide range of application, FCS measurements are restricted to monitoring at only one volume element defined by both a focused laser beam and a pinhole. Although there have been a few reports on FCS experiments with multiple detection areas,[4–6] further advances in the number of detection areas, sensitivity, time resolution, and methods are required.

Heterogeneous structures of cell surfaces and the motion of membrane-binding molecules are thought to be dynamic and presumed to modulate the formation of cell-signaling molecular complexes at the membranes. Hence, simultaneous FCS measurement with multiple detection areas would be an attractive tool for understanding of the heterogeneous diffusion properties of cell membranes and such cell signaling.

Recently, some research groups reported total internal reflection fluorescence correlation spectroscopy[7–11] (TIR-FCS) and its application to living cells.[11] Although the limited-time temporal resolution of 4 ms, electron-multiplying CCD (EMCCD)-camera-based multipoint TIR-FCS measurement was achieved.[12] Extension of the multipoint FCS system will be spatially resolved FCS such as image correlation spectroscopy (ICS), however the temporal resolution should be improved[13] (see more detailed in the review article in Ref. 14). In previous work, we also reported the multipoint FCS measurement made by confocal laser-scanning microscopy. The detection areas were focused in the cytoplasm that located deeper from the plasma membrane though the measurements were not completely simultaneously.[15]

In this paper, we describe the high temporal resolution of multipoint TIR-FCS (M-TIR-FCS). TIR illumination produces an evanescent field. The intensity decreases exponentially along the optical axis but is widely spreading on the surface. Therefore, as shown in Fig. 1(a), multipoint FCS detection areas in the evanescent field were achieved by putting multiple optical fibers on the image plane.

The optics of M-TIR-FCS is based on an objective-type TIR-FCS, which is combined with objective-type total internal reflection fluorescence microscopy (TIRFM, TE2000, Nikon) with a $\times 100$ oil-immersion objective [Plan Apo, numerical aperture (NA) 1.49, Nikon] for TIR illumination and a 488-nm semiconductor laser (488-20CDRH, Coherent, California) for the excitation. On the other hand, a bundle of seven multimode fibers with a 50-μm-diam core (Seiko-Giken, Chiba, Japan) to produce seven detection areas in the evanescent field was placed on an image plane in its decection port. Seven photomultiplier tubes (PMTs, H7421, Hamamatsu Photonics K. K., Shizuoka, Japan) to detect fluorescence signals in parallel through each optical fiber and a multichannel correlator (Hamamatsu Photonics K. K.) to simultaneously calculate seven autocorrelation functions were set up as shown in Fig. 1(b). The sensitivity of the PMT is a little lower than that of an avalanche photodiode (APD), but the price of PMT is lower than that of the APD and the PMT has lager detection area so that it is easy to align; these properties are benefits for a multiple-detection system.

Address all correspondence to Masataka Kinjo, Hokkaido University, Laboratory of Molecular Cell Dynamics, Faculty of Advanced Life Science, Sapporo 001-0021, Japan; Tel: +81-11-706-9005; E-mail: kinjo@sci.hokudai.ac.jp

1083-3668/2009/14(1)/014030/4/$25.00 © 2009 SPIE

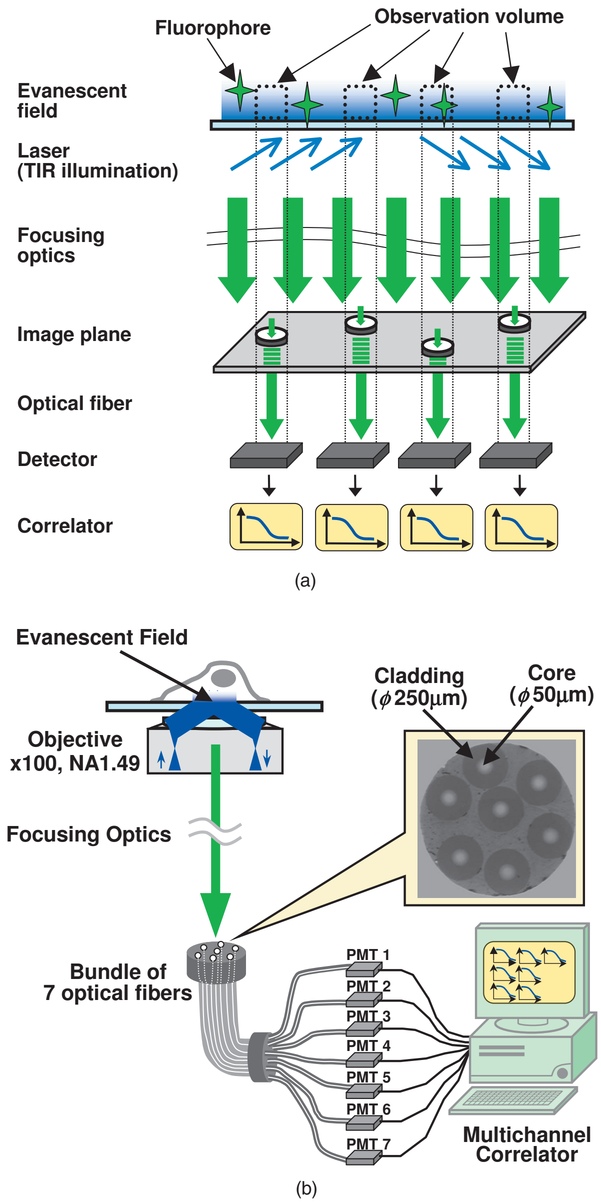

Fig. 1 (a) Schematic of multipoint FCS with TIR-FM. Though this figure shows four detection areas, we produced seven detection areas, as shown in (b). (b) Diagram of M-TIR-FCS setup for cellular observation.

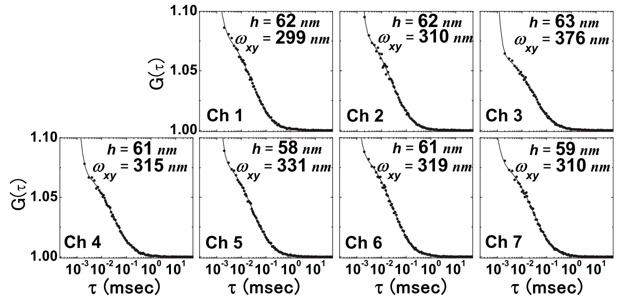

Fig. 2 Control experiments for determination of the structure parameters at each detection area of M-TIR-FCS. Seven autocorrelation functions (dotted line) were simultaneously obtained by measuring 100-nM FITC in 10-mM Tris buffer solution (pH 8.0) at seven points in the evanescent field. The fits are indicated by solid lines. The values of the height (h) and radius (ωxy) in each channel obtained by fitting are shown in each panel. The units of h and ωxy are nanometers (nm). The averages ± standard deviation of τ_z for each channel are, 3.2±0.2, 3.2±0.3, 3.3±0.3, 3.1±0.3, 2.9±0.3, 3.1±0.2, and 2.9±0.1 μs. The averages of h for each channel are 62±1.6, 62±2.5, 63±3.2, 61±2.0, 58±3.6, 61±1.9, and 59±1.4 nm. The averages of ω_{xy} for each channel are 299±4.0, 310±14.0, 376±10.5, 315±4.0, 331±10.0, 319±4.1, and 310±1.6 nm, for Ch 1 to Ch 7, respectively. Results were the average of five measurements of a total duration time of 30 s (10 loops of 3 s). The average count rates are 96.6, 104.3, 147.4, 118.6, 120.5, 104.6, and 95.6 kcounts/s, background is 0.1 kcounts/s and the average count per molecules (CPM) is about 18 kcounts/s.

For the calibration control experiments on 100-nM fluorescein (FITC) in 10-mM Tris buffer (pH 8.0) were carried out according to previous study.[11] By monitoring seven detection areas at the same time, seven individual fluorescence autocorrelation functions (FAFs) $G(\tau)$ were acquired online with a digital multichannel correlator (Hamamatsu Photonics K. K., Shizuoka, Japan). As shown in Fig. 2, seven autocorrelation functions (dotted line) were simultaneously obtained. To calibrate the size distribution among the seven detection volumes, fitting by a one-component model[9,11] (solid lines), [Eq. (1)], was conducted to obtain the height (h) and the radius (ω_{xy}) of each detection volume. The structure parameter is defined[9] by $\omega = h/\omega_{xy}$.

$$G(\tau) = \frac{\langle I(t)\cdot I(t+\tau)\rangle}{\langle I(t)\rangle^2}$$
$$= 1 + \frac{\gamma}{N}\left[1 + \frac{p}{1-p}\exp\left(-\frac{\tau}{\tau_t}\right)\right]\left(1 + \frac{\omega^2\tau}{\tau_z}\right)^{-1}$$
$$\times\left[\left(1 - \frac{\tau}{2\tau_z}\right)w\left(i\sqrt{\frac{\tau}{4\tau_z}}\right) + \sqrt{\frac{\tau}{\pi\tau_z}}\right]. \tag{1}$$

The analysis yielded diffusion time along the z axis, $\tau_z = 3.5\ \mu$s, which shows that M-TIR-FCS has a 3-μs time resolution at least. However, time resolution is not clear in this study because the time resolution should take into account the resolution of the detector, amplifier, and correlator system. In a small lag time range, a high peak signal were observed and fitted by the triplet term by using Eq. (1). Though the after pulse could be effected to the signal at small lag time, the effect will be small composed to the diffusion signal part. The difference in the values of h and ω_{xy} might be due to the deviation of the core sizes of optical fibers, the z axis position at the image plane, and alignment of the fibers (Fig. 2). The height and radius of the detection volumes were about 60 and 330 nm, respectively. These parameters were influenced by TIR angle as follows. According to the increase in the TIR angle from critical angle, τ_z decreases to 4.3 ± 0.9, 3.8 ± 0.8, 3.1 ± 0.5, and $2.6\pm0.3\ \mu$s, and h decreases to 72 ± 7.6, 67 ± 7.9, 60 ± 4.5, and 56 ± 3.5 nm, respectively. On the other hand ω_{xy} is constant to 387 ± 33.4, 386 ± 28.7, 387 ± 30.5, and 385 ± 31.6 nm. Finally, N decreases 19.6 ± 0.9, 19.8 ± 1.0, 19.1 ± 1.1, and 18.0 ± 2.0. The distances between each core of the optical fibers on the image

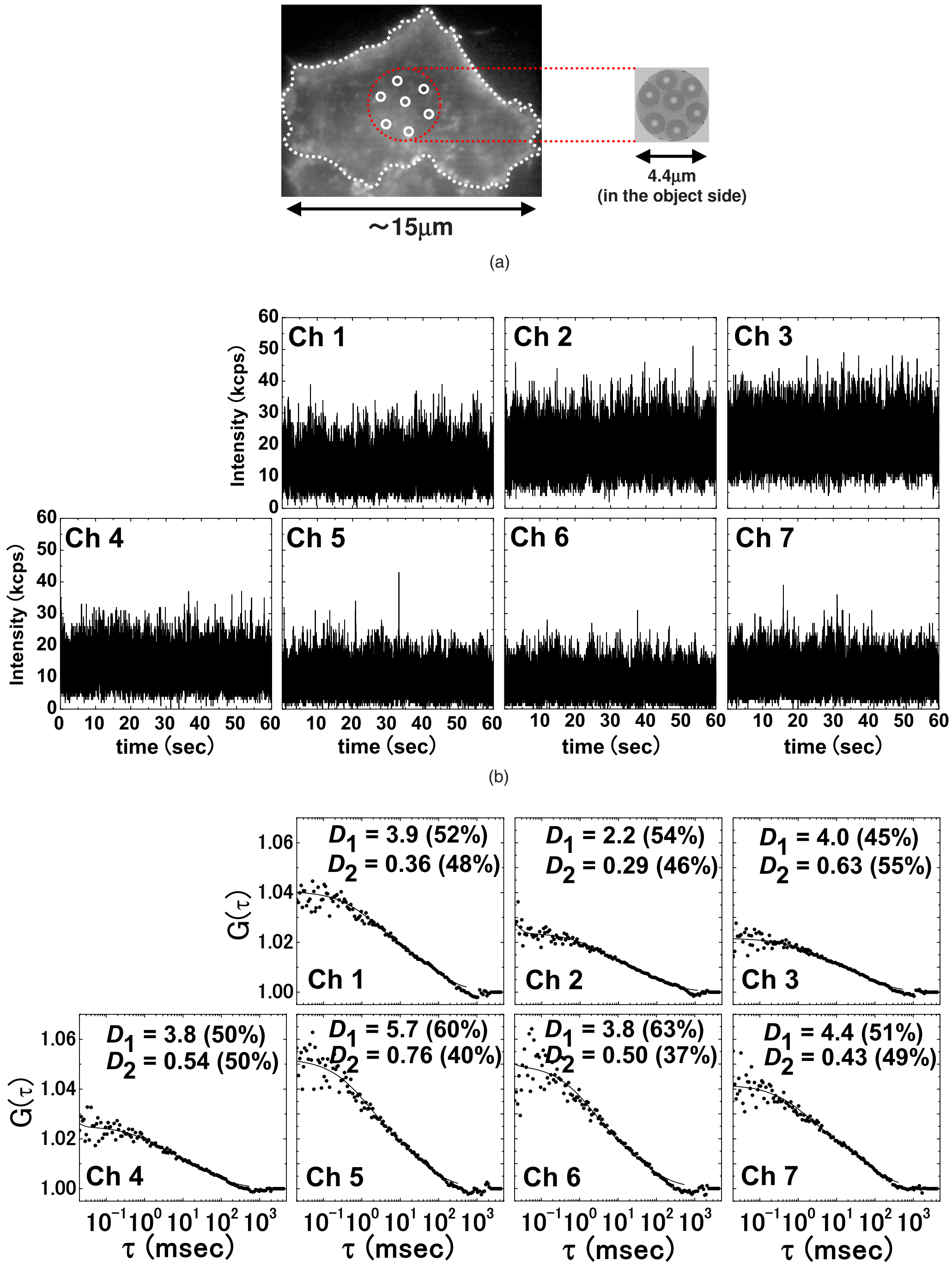

Fig. 3 M-TIR-FCS measurements of membrane-binding proteins in living cells; (a) seven detection areas of M-TIR-FCS in the cell membrane of a COS7 cell expressing mGFP-F; (b) seven time courseS of fluorescence intensity during measurement; (c) seven autocorrelation functions for the membrane-binding proteins, mGFP-F, in a living COS7 cell simultaneously measured by M-TIR-FCS. Measured autocorrelation functions (dotted line) are fitted by a two-component model (solid lines). Diffusion constants (D) and their fractions are shown in the panels. All diffusion constants are described in units of 10^{-8} cm^2/s. Results were the average of three measurement of total duration time of 60 s (20 loops of 3 s). Excitation intensity of laser power was 0.084 $\mu W/\mu m^2$.

plane was about 250 μm, as shown in Fig. 1(b). In this system, the distances between each M-TIR-FCS detection spots were about 2.5 μm because we used a $\times 100$ objective. The distance of 2.5 μm was distant enough for the observation area of 660 nm not to detect crosstalk signals from neighboring detection spots. Also, the cross-correlation between signal from each spot was not detected (data not shown). From these results, we confirmed that M-TIR-FCS worked successfully.

Next, we carried out measurement of membrane-binding fluorescent proteins expressed in a living COS7 cell using M-TIR-FCS. Expression vectors encoding farnesylated monomeric-type EGFP A206K variants, which are abbreviated mGFP-F, were constructed by mutating sequences of pEGFP-F (Clontech) with site-directed mutagenesis (Quick-Change, Stratagene). For M-TIR-FCS measurement, COS7 cells were grown on glass-based dishes (ϕ 12 mm, Asahi Technoglass, Chiba, Japan) 2 days before measurements. The cells were transiently transfected with 0.5 μg of plasmid DNA of mGFP-F and 4.0 μg of optifect (Invitrogen) 17 h before M-TIR-FCS measurements. The left photograph in Fig. 3(a) shows TIRFM image of a COS7 cell expressing farnesylated monomeric type (A206K) enhanced GFP, mGFP-F. The broken white line shows the border of the plasma membrane of a COS7 cell attached to the glass surface. The width of the cell is about 15 μm. The right photograph in Fig. 3(a) shows the end face of the bundle of optical fibers used as seven pinholes. The value 4.4 μm is the length of the projected image in the object port. Figure 3(b) shows the seven autocorrelation functions (dotted lines) obtained by M-TIR-FCS of mGFP-F in the cellular membrane of a COS7 cell and its fitting results with a lateral diffusion parallel to the surface and three dimensional diffusion through evanescent profile[11] [Eq. (2) (solid line)].

$$G(\tau) = 1 + \frac{\gamma}{N}\left\{F_1\left(1 + \frac{\omega^2\tau}{\tau_{1,z}}\right)^{-1}\left[\left(1 - \frac{\tau}{2\tau_{1,z}}\right)\mathrm{w}\left(i\sqrt{\frac{\tau}{4\tau_{1,z}}}\right) + \sqrt{\frac{\tau}{\pi\tau_{1,z}}}\right] + F_2\left(1 + \frac{\tau}{\tau_{2,xy}}\right)^{-1}\right\}, \qquad (2)$$

where F_1 and F_2 are each fraction, respectively.

The time range of the correlation function is much slower than that obtained by measurements of fluorescein in aqueous solution. These results show the TIR-FCS covers a wide range of diffusion time induced by large molecular complex in cell membrane. Diffusion constants of mGFP-F in the cell membrane were calculated in the same way as described in a previous report.[11] The 3-D diffusion can be related to free-moving protein in cytosol because the obtained diffusion constant is comparative with previous report.[11] The difference in values of D_2 may reflect the heterogeneous structure of cellular membranes, and its average value is almost the same as the result in a previous work.[11] At the large lag time, the measurement curves seem to decay much faster than the model. This may be the result of the instability of the measurement conditions; this should be answered in near future.

We reported simultaneous diffusion measurement at multiple tiny areas close to surfaces in not only aqueous solution but also in live cells using multipoint FCS with a wide time resolution from the microsecond to the millisecond range. Because the mGFP-F membrane-binding protein we measured here is a model protein, the variation of its diffusion rate on membranes would still be small. Thus, M-TIR-FCS can be a powerful technique for the study of more complex and heterogeneous specimen, i.e., membrane-receptor complex in live cells. Furthermore, the spatial cross-correlation method[16] would be applicable to this system and make M-TIR-FCS versatile and more oriented toward FCS imaging.[17] A much more interesting application would be to exploit simultaneously the spatial and temporal correlation between different measurement positions. This could enable us to measure drift, diffusional anisotropy, direction flow, and other effects. However, these applications should be performed in the near future.

Acknowledgments

This research was partly supported by Grand-in-Aid for Scientific Research (B) 15370062 and (A) 18207010 from the Japan Society for the Promotion of Science (JSPS), and No. 19058001 in Priority Area “Protein Community,” No. 19021001 “Life Surveyor,” and No. 19038001 “Nuclear Dynamics.” MK kindly thanks Yutaka Hasegawa, Masami Sugie, and Hisashi Matsui (Hamamatsu Photonics K. K., Co., Ltd.) for supporting the real-time multipoint FCS system

References

1. R. Rigler, Ü. Mets, J. Widengren, and P. Kask, “Fluorescence correlation spectroscopy with high count rate and low background: analysis of translational diffusion,” *Eur. Biophys. J.* **22**, 169–175 (1993).
2. M. Kinjo and R. Rigler, “Ultrasensitive hybridization analysis using fluorescence correlation spectroscopy,” *Nucleic Acids Res.* **23**, 1795–1799 (1995).
3. K. Bacia, S. A. Kim, and P. Schwille, “Fluorescence cross-correlation spectroscopy in living cells,” *Nat. Methods* **3**(2), 83–89 (2006).
4. H. Blom, M. Johansson, A.-S. Hedman, L. Lundberg, A. Hanning, S. Hård, and R. Rigler, “Parallel fluorescence detection of single biomolecules in microarrays by a diffractive-optical-designed 2×2 fan-out element,” *Appl. Opt.* **41**, 3336–3342 (2002).
5. M. Gösch, A. Serov, T. Anhut, T. Lasser, A. Rochas, P.-A. Besse, R. S. Popovic, H. Blom, and R. Rigler, “Parallel single molecule detection with a fully integrated single-photon 2×2 CMOS detector array,” *J. Biomed. Opt.* **9**, 913–921 (2004).
6. M. Burkhardt and P. Schwille, “Electron multiplying CCD based detection for spatially resolved fluorescence correlation spectroscopy,” *Opt. Express* **14**, 5013–5020 (2006).
7. N. L. Thompson, T. P. Burghardt, and D. Axelrod, “Measuring surface dynamics of biomolecules by total internal-reflection fluorescence with photobleaching recovery or correlation spectroscopy,” *Biophys. J.* **33**, 435–454 (1981).
8. K. Hassler, T. Anhut, R. Rigler, M. Gösch, and T. Lasser, “High count rates with total internal reflection fluorescence correlation spectroscopy,” *Biophys. J.* **88**, L01–L03 (2005).
9. K. Hassler, M. Leutenegger, P. Rigler, R. Rao, R. Rigler, M. Gösch, and T. Lasser, “Total internal reflection fluorescence correlation spectroscopy (TIR-FCS) with low background and high count-rate per molecule,” *Opt. Express* **13**, 7415–7423 (2005).
10. J. Ries, E. P. Petrov, and P. Schwille, “Total internal reflection fluorescence correlation spectroscopy: effects of lateral diffusion and surface generated fluorescence,” *Biophys. J.* **95**, 390–399 (2008).
11. Y. Ohsugi, K. Saito, M. Tamura, and M. Kinjo, “Lateral mobility of membrane-binding proteins in living cells measured by total internal reflection fluorescence correlation spectroscopy,” *Biophys. J.* **91**, 3456–3464 (2006).
12. B. Kannan, L. Guo, T. Sudhaharan, S. Ahmed, I. Maruyama, and T. Wohland, “Spatially resolved total internal reflection fluorescence correlation microscopy using an electron multiplying charge-coupled device camera,” *Anal. Chem.* **79**, 4463–4470 (2007).
13. D. R. Sisan, R. Arevalo, C. Graves, R. McAllister, and J. S. Urbach, “Spatially resolved fluorescence correlation spectroscopy using a spinning disk confocal microscope,” *Biophys. J.* **91**, 4241–4252 (2006).
14. D. L. Kolin and P. W. Wiseman, “Advances in image correlation spectroscopy: measuring number densities, aggregation states, and dynamics of fluorescently labeled macromolecules in cells,” *Cell Biochem. Biophys.* **49**, 141–164 (2007).
15. Y. Takahashi, R. Sawada, K. Ishibashi, S. Mikuni, and M. Kinjo, “Analysis of cellular functions by multipoint fluorescence correlation spectroscopy,” *Curr. Pharm. Biotechnol.* **6**, 159–165 (2005).
16. D. J. LeCaptain and A. V. Orden, “Two-beam fluorescence cross-correlation spectroscopy in an electrophoretic mobility shift assay,” *Anal. Chem.* **74**, 1171–1176 (2002).
17. Z. Gryczynski, “FCS imaging—a way to look at cellular processes,” *Biophys. J.* **94**, 1943–1944 (2008).